*Structural Engineering and Mechanics, Vol. 10, No. 1 (2000) 67-79*
DOI: http://dx.doi.org/10.12989/sem.2000.10.1.067



# Load-carrying capacities and failure modes of scaffold-shoring systems, Part II: An analytical model and its closed-form solution

Y.L. Huang† and Y.G. Kao‡

*Department of Civil Engineering, Chung-Hsing University, Taichung, 40227 Taiwan, R.O.C.*

D.V. Rosowsky†

*Department of Civil Engineering, Clemson University, Clemson, SC 29634-0911, U.S.A.*

**Abstract.** Critical loads and load-carrying capacities for steel scaffolds used as shoring systems were compared using computational and experimental methods in Part I of this paper. In that paper, a simple 2-D model was established for use in evaluating the structural behavior of scaffold-shoring systems. This 2-D model was derived using an incremental finite element analysis (FEA) of a typical complete scaffold-shoring system. Although the simplified model is only two-dimensional, it predicts the critical loads and failure modes of the complete system. The objective of this paper is to present a closed-form solution to the 2-D model. To simplify the analysis, a simpler model was first established to replace the 2-D model. Then, a closed-form solution for the critical loads and failure modes based on this simplified model were derived using a bifurcation (eigenvalue) approach to the elastic-buckling problem. In this closed-form equation, the critical loads are shown to be function of the number of stories, material properties, and section properties of the scaffolds. The critical loads and failure modes obtained from the analytical (closed-form) solution were compared with the results from the 2-D model. The comparisons show that the critical loads from the analytical solution (simplified model) closely match the results from the more complex model, and that the predicted failure modes are nearly identical.

**Key words:** scaffolds; shores; critical loads; elastic buckling; failure modes.

## 1. Introduction

Steel scaffold shoring systems are a common type of falsework. The collapse of a shoring system can have disastrous consequences on a construction project. During recent years, the load-carrying capacity of scaffold shoring systems has been the subject of both computational and experimental research. Experimental studies such as those reported by Yen *et al.* (1997) and Huang *et al.* (1999) have considered full-scale tests of scaffold systems up to five stories in height. Jan (1987), Peng *et al.* (1996), and Huang *et al.* (1999) have developed analytical procedures for determining the critical loads of scaffold systems, often using finite element analysis (FEA). In recent studies, simple design guidelines have been suggested for determining the load-carrying capacity of a scaffold shoring

† Associate Professor
‡ Graduate Student

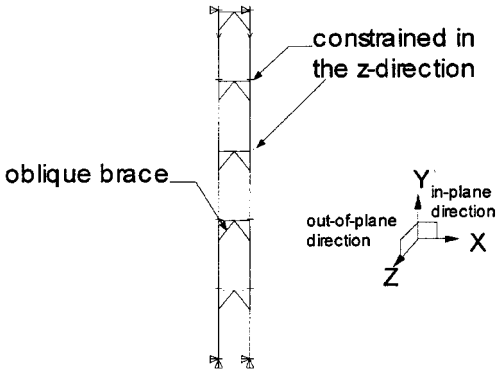


Fig. 1 2-D model

system. So far, however, little is known about the relationship between the critical load and the number of stories, material properties, and section properties of the scaffold shores. In Part I of this paper, a 2-D model (shown in Fig. 1) was developed by simplifying a typical complete scaffold-shoring system through a stepwise analysis. In that study, it was shown that the relatively simple 2-D model was capable of predicting critical loads and failure modes for the entire scaffold system. Part I of this paper also recommended the 2-D model for use in further computational analysis of complete scaffold-shoring systems.

The objective of this paper is to develop the theoretical basis for the 2-D model. This is accomplished through the derivation of a closed-form solution for this model. To simplify the analysis, the 2-D model is first simplified even further. The analytical model is validated using computational methods (FEA) to ensure that it predicts the same structural behavior, i.e., critical loads and failure modes, as the 2-D model. Then, a closed-form solution to the analytical model is derived using a bifurcation approach (eigenvalue method) to the elastic-buckling problem.

## 2. Analytical model

In deriving a closed-form solution to the 2-D model, an even simpler analytical model is first established in order to simplify the analysis procedure. The sizes and material properties of the scaffolds in this paper are the same as those in Part I of this paper (Huang *et al.* 1999). They are shown in Fig. 2 and are as follows:

section area $A = 2.73$ cm$^2$
moment of inertia $I_A = 5.43$ cm$^4$
$E = 204$ GPa
$F_y = 515$ MPa
$F_u = 645$ MPa

In this paper, the analytical model consists of only one horizontal and two vertical bars. In the 2-D model (see Fig. 1), the horizontal bar was connected by two oblique braces, increasing the strength of the horizontal bar considerably. Thus, the horizontal bar with the two oblique braces in the 2-D model was modeled as a single rigid horizontal bar in the analytical model. Since the oblique braces can also increase the stiffness of the vertical bars, the moment of inertia of the

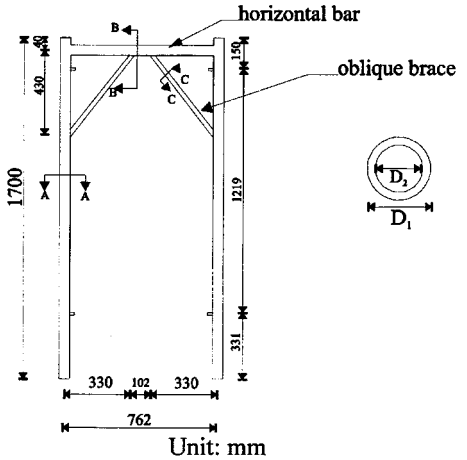


Unit: mm

| Section | $D_1$(mm) | $D_2$(mm) | Area(mm$^2$) |
|---|---|---|---|
| A | 42.01 | 37.65 | 273.1 |
| B | 42.01 | 37.65 | 273.1 |
| C | 26.37 | 22.5 | 148.5 |

Fig. 2 Shape and sizes of scaffold used in this study

vertical bars in the analytical model must be greater than in the 2-D model ($I$). The moment of inertia of the vertical bar in the analytical model was assumed to be $\alpha I$ (in which $\alpha > 1$) to reflect the presence of the oblique braces. Therefore, the initial analytical model can be described schematically as shown in Fig. 3. The value for the constant $\alpha$ will be determined by comparing the computational results obtained from the 2-D and analytical models.

Since the oblique braces serve to increase the stiffness of the vertical bars, the value of $\alpha$ should

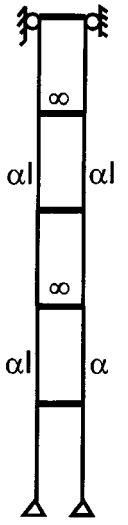


Fig. 3 Initial analytical model

Table 1 Computational critical loads from analytical model (with $\alpha$=1) and 2-D model

| No. of stories | (1) $P_{cr.}$ of the Analytical model with $\alpha$=1 (N) | (2) $P_{cr.}$ of the 2-D model (N) | (3)=(2)/(1) |
|---|---|---|---|
| 2 | 46500 | 66530 | 1.431 |
| 3 | 37020 | 54860 | 1.482 |
| 4 | 32170 | 48180 | 1.498 |
| 5 | 29180 | 43930 | 1.505 |
| 6 | 27140 | 40990 | 1.510 |
| 7 | 25650 | 38880 | 1.516 |
| 8 | 24520 | 37300 | 1.521 |
| 9 | 23630 | 36110 | 1.528 |
| 10 | 22930 | 35200 | 1.535 |
| 11 | 22360 | 34490 | 1.542 |
| 12 | 21900 | 33930 | 1.549 |
| 13 | 21520 | 33490 | 1.556 |
| 14 | 21200 | 33140 | 1.563 |
| 15 | 20940 | 32860 | 1.569 |
| 16 | 20720 | 32640 | 1.575 |
| 17 | 20540 | 32460 | 1.580 |
| 18 | 20390 | 32310 | 1.585 |
| 19 | 20260 | 32190 | 1.589 |
| 20 | 20150 | 32090 | 1.593 |

In column (3), $n$ = 19, mean = 1.538, $\sigma_n$ = 0.041, $\sigma_{n-1}$ = 0.042

be greater than 1. To determine the value of $\alpha$, first assume that $\alpha$ is equal to 1 and then determine the critical loads for scaffold systems of 2-20 in height, using both the 2-D and analytical models. These two families of critical loads are listed in Table 1 and are shown graphically in Fig. 4. From this figure and table, it can be seen that all of the critical loads obtained using the 2-D model are greater than those obtained using the analytical model. The ratios of the former to the latter, which are also listed in Table 1, range from 1.43 to 1.59 with an average of 1.54 and a coefficient of variation (COV) of 0.04. The very small COV suggests relatively little variability; i.e., the ratios are all very near to the same value. In Part I of this paper, it was shown that the critical loads are almost linearly proportional to the moment of inertia of the vertical bar. Therefore, $\alpha$ = 1.54 was adopted to account for the effect of the oblique braces. The analytical model with $\alpha$ = 1.54 was again used to calculate the critical loads. These critical loads are listed in Table 2, together with the critical loads obtained from the 2-D model. From this table, it can be seen that the computational critical loads from the analytical model with $\alpha$ = 1.54 are now very similar to those from the 2-D model. Therefore, a vertical bar with an oblique brace in the 2-D model can be replaced by a single vertical bar whose moment of inertia is 1.54 times as large as the original moment inertia. The final analytical model is shown in Fig. 5.

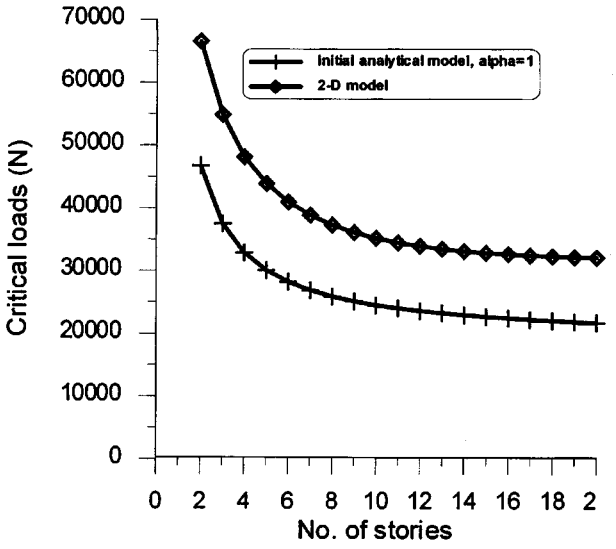


Fig. 4 Computational critical loads from 2-D model and the temporary analytical model (with $\alpha$=1)

Table 2 Computational critical loads from analytical model (with $\alpha$=1.54) and 2-D model

| No. of stories | (1) $P_{cr.}$ of the analytical model with $\alpha$=1.54 (N) | (2) $P_{cr.}$ of the 2-D model (N) | (3)=(2)/(1) |
|---|---|---|---|
| 2 | 71610 | 66530 | 1.076 |
| 3 | 57010 | 54860 | 1.039 |
| 4 | 49540 | 48180 | 1.028 |
| 5 | 44940 | 43930 | 1.023 |
| 6 | 41800 | 40990 | 1.020 |
| 7 | 39500 | 38880 | 1.016 |
| 8 | 37760 | 37300 | 1.012 |
| 9 | 36390 | 36110 | 1.008 |
| 10 | 35310 | 35200 | 1.003 |
| 11 | 34430 | 34490 | 0.998 |
| 12 | 33730 | 33930 | 0.994 |
| 13 | 33140 | 33490 | 0.990 |
| 14 | 32650 | 33140 | 0.985 |
| 15 | 32250 | 32860 | 0.981 |
| 16 | 31910 | 32640 | 0.978 |
| 17 | 31630 | 32460 | 0.974 |
| 18 | 31400 | 32310 | 0.972 |
| 19 | 31200 | 32190 | 0.969 |
| 20 | 31030 | 32090 | 0.967 |

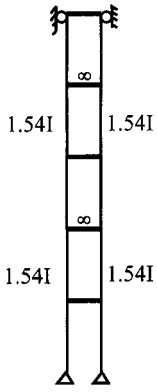


Fig. 5 Final analytical model

## 3. Derivation of the closed-form solution for critical load

The following assumptions are made for the bifurcation approach to derive the closed-form solution for the critical loads:

(1) All members are in the elastic range.

(2) The analytical model buckles in the in-plane direction.

(3) The analytical model buckles at the lowest (first) story.

(4) According to assumption (3), sidesway of the lowest story is given by $\Delta$, and sidesway of any other story is $\Delta/(n-1)$, as shown in Fig. 6.

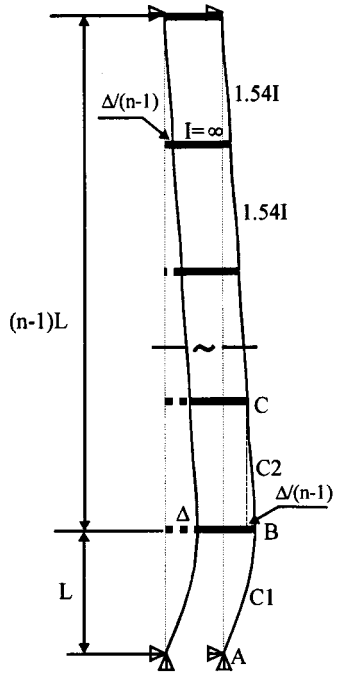


Fig. 6 Assumption of sidesway for analytical model

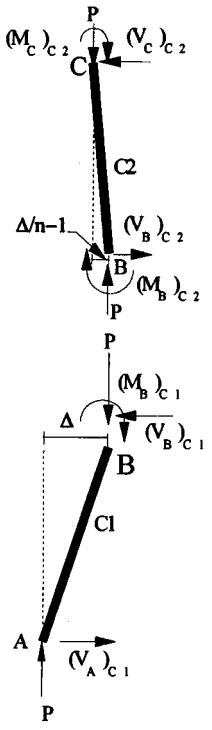


Fig. 7 Free-body diagram of columns AB and BC

Using the slope-deflection method (refer to Chen *et al.* 1987) and according to the free-body diagram shown in Fig. 7, the moments at both ends of columns *AB* and *BC* (see Fig. 6) are:

Column AB:

$$(M_A)_{c1}=\left(\frac{E\alpha I}{L}\right)\left[S_{ii}\theta_A-(S_i+{}_iS_{ij})\frac{\Delta}{L}\right]=0 \tag{1}$$

$$(M_B)_{c1}=\left(\frac{E\alpha I}{L}\right)\left[S_{ij}\theta_A-(S_i+{}_iS_{ij})\frac{\Delta}{L}\right]=\left(\frac{E\alpha I}{L}\right)\left[-\left(S_i-{}_i\frac{S_{ij}^2}{S_{ii}}\right)\frac{\Delta}{L}\right] \tag{2}$$

Column BC:

$$(M_B)_{c2}=\left(\frac{E\alpha I}{L}\right)\left[(S_i+{}_iS_{ij})\frac{\left(\frac{\Delta}{N-1}\right)}{L}\right] \tag{3}$$

$$(M_C)_{c2}=\left(\frac{E\alpha I}{L}\right)\left[(S_i+{}_iS_{ij})\frac{\left(\frac{\Delta}{N-1}\right)}{L}\right]=(M_B)_{c2} \tag{4}$$

in which

$\alpha$=1.45

$$S_{ii}=\frac{kL\sin kL-(kL)^2\cos kL}{2-2\cos kL-kL\sin kL} \tag{5}$$

$$S_{ij}=\frac{(kL)^2-kL\sin kL}{2-2\cos kL-kL\sin kL} \tag{6}$$

where

$$kL=\pi\sqrt{\frac{P}{P_e}} \tag{7}$$

and

$$P_e=\frac{\pi^2E(\alpha I)}{L^2} \tag{8}$$

For joint equilibrium at B

$$\frac{(M_B)_{c1}+P\Delta}{L}=\frac{(M_B)_{c2}+(M_C)_{c2}-P\frac{\Delta}{N-1}}{L}$$

$$(M_B)_{c1}-2(M_B)_{c2}+P\Delta\frac{N}{N-1}=0 \tag{9}$$

From Eqs. (7) and (8)

$$P\Delta\left(\frac{E\alpha I}{L}\right)(kL)^2\frac{\Delta}{L} \tag{10}$$

Substituting Eqs. (2), (3) and (10) into Eq. (9) results in:

$$\left(\frac{E\alpha I}{L}\right)\left[-\left(S_i-{}_i\frac{S_{ij}^2}{S_i}\right)-2\frac{S_i+{}_iS_{ij}}{N-1}+\frac{N}{N-1}(kL)^2\right]\frac{\Delta}{L}=0$$

At bifurcation, we have

$$\left[(N-1)\left(\frac{S_{ij}^2}{S_i}-S_i\right)-2(S_i+{}_iS_{ij})+N(kL)^2\right]=0 \tag{11}$$

Eq. (11) can be simplified (as shown in the Appendix) to:

$$2(N-1)(1-\sec kL)+NkL\tan kL-\tan^2kL=0 \tag{12}$$

Eq. (12) is now the analytical (closed-form) solution for the critical load based on the analytical model. In this closed-form equation, critical load is a function of the number of stories, material properties and section properties. The critical loads calculated using Eq. (12) are listed in Table 3.

## 4. Comparisons of the analytical solutions and computational solutions

Analytical (closed-form) solutions were obtained using the bifurcation analysis described in the

Table 3 Critical loads based on closed-form equation using analytical model

| No of stories | $kL$ from Eq. 12 | $P_{cr.}$ from Eq. 12 ($N$) |
|---|---|---|
| 2 | 2.470 | 72030 |
| 3 | 2.212 | 57770 |
| 4 | 2.071 | 50640 |
| 5 | 1.981 | 46330 |
| 6 | 1.919 | 43470 |
| 7 | 1.873 | 41410 |
| 8 | 1.838 | 39890 |
| 9 | 1.811 | 38710 |
| 10 | 1.788 | 37750 |
| 11 | 1.770 | 36990 |
| 12 | 1.754 | 36310 |
| 13 | 1.741 | 35790 |
| 14 | 1.729 | 35290 |
| 15 | 1.719 | 34880 |
| 16 | 1.710 | 34530 |
| 17 | 1.702 | 34200 |
| 18 | 1.695 | 33910 |
| 19 | 1.689 | 33680 |
| 20 | 1.683 | 33430 |

previous section. The computational solutions were obtained using FEA of the 2-D model. The analytical and computational critical loads and failure modes are compared in the following sections.

### 4.1. Comparison of critical loads

Critical loads obtained from the closed-form solution of the analytical model, the computational solution obtained using FEA of the same analytical model, and the computational solution from the 2-D model are listed together in Table 4, and are graphed in Fig. 8. From the table and figure, it can be seen that the three families of critical loads are very close to one another. The decreasing trend with number of stories is also similar for the three curves; the maximum difference in the magnitudes of the critical loads does not exceed 8%. The closed-form critical loads are slightly higher than the computational critical loads, most likely due to differences in the sidesway assumptions between the analytical and the computational models. Since these differences are very small, the closed-form solution of the analytical model given by Eq. (12) is accepted as the closed-form solution to the 2-D model.

### 4.2. Comparison of failure modes

Consider a 5-story high scaffold system as an example. The failure modes from the computational and analytical models are shown in Fig. 9. In both cases, buckling occurred in the first (lowest) story in the in-plane direction, and the largest displacements occurred at the top of the first (lowest)

Table 4 Critical loads based on closed-form equation using analytical mode; FEA method using analytical model; and FEA method using 2-D model

| No. of stories | (1) $P_{cr.}$ based on Eq. 12 Using the analytical model ($N$) | (2) $P_{cr.}$ based on FEA method using the analytical model (N) | (3) $P_{cr.}$ based on FEA method using the 2-D model (N) | (4) = (1)/(2) | (5) = (1)/(3) |
|---|---|---|---|---|---|
| 2 | 72030 | 71610 | 66530 | 1.01 | 1.08 |
| 3 | 57770 | 57010 | 54860 | 1.01 | 1.05 |
| 4 | 50640 | 49540 | 48180 | 1.02 | 1.05 |
| 5 | 46330 | 44940 | 43930 | 103 | 1.06 |
| 6 | 43470 | 41800 | 40990 | 1.04 | 1.06 |
| 7 | 41410 | 39500 | 38880 | 1.06 | 1.07 |
| 8 | 39890 | 37760 | 37300 | 1.06 | 1.07 |
| 9 | 38710 | 36390 | 36110 | 1.06 | 1.07 |
| 10 | 37750 | 35310 | 35200 | 1.07 | 1.07 |
| 11 | 36990 | 34430 | 34490 | 1.07 | 1.07 |
| 12 | 36310 | 33730 | 33930 | 1.08 | 1.07 |
| 13 | 35790 | 33140 | 33490 | 1.08 | 1.07 |
| 14 | 35290 | 32650 | 33140 | 1.08 | 1.07 |
| 15 | 34880 | 32250 | 32860 | 1.08 | 1.06 |
| 16 | 34530 | 31910 | 32640 | 1.08 | 1.06 |
| 17 | 34200 | 31630 | 32460 | 1.08 | 1.05 |
| 18 | 33910 | 31400 | 32310 | 1.08 | 1.05 |
| 19 | 33680 | 31200 | 32190 | 1.08 | 1.05 |
| 20 | 33430 | 31030 | 32090 | 1.08 | 1.04 |

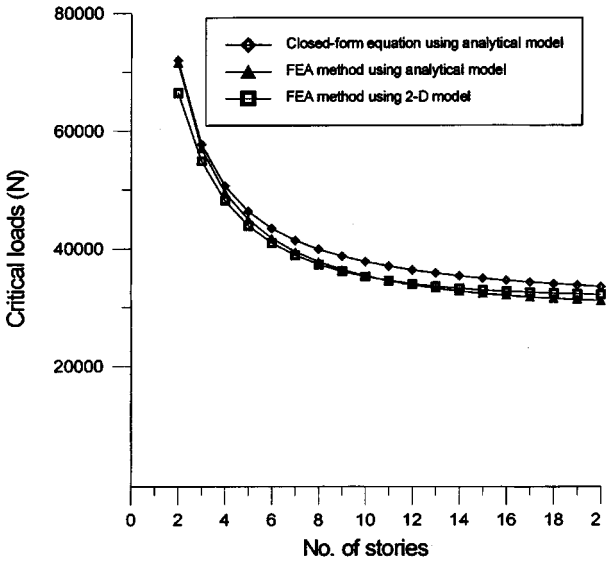


Fig. 8 Critical loads based on closed-form equation using analytical model; FEA method using analytical model; and FEA method using 2-D model

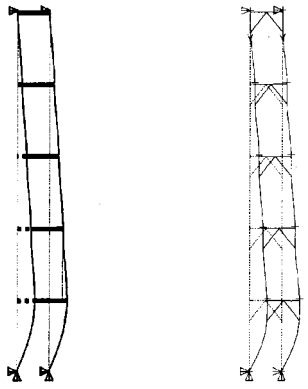

Analytical model 2-D model

Fig. 9 Failure modes of analytical and 2-D models

Table 5 Computational sidesway of each floor in a 5-story system based on FEA method using analytical model

| No. of stories, $i$ | Sidesway $x_i$ | Inter-story drift $\lvert x_i-x_{i+1}\rvert$ | Inter-story drift ratio $\lvert x_i-x_{i+1}\rvert/\lvert x_1-x_0\rvert$ |
|---|---|---|---|
| 0 | 0 | 1 | 1 |
| 1 | 1 | 0.2312 | 0.2312 |
| 2 | 0.7688 | 0.2472 | 0.2472 |
| 3 | 0.5216 | 0.2577 | 0.2577 |
| 4 | 0.2639 | 0.2639 | 0.2639 |
| 5 | 0 | | |

$|x_1-x_0|=1$

story. The sidesways at the top of each story obtained from the computational model are listed in Table 5. This table indicates that the sidesway of the top of the lowest story is nearly four times the sidesway of any other story. This serves to validate the previous sidesway assumption made in the analytical model.

The comparisons of both failure modes and critical loads obtained using the analytical and computational models suggest that the 2-D model developed in Part I of this paper can be replaced by the simpler analytical model proposed here. The closed-form solutions to this analytical model can then be accepted as the theoretical solution to the 2-D model.

## 5. Conclusions

In Part I of this paper, the relationship between the load-carrying capacity and number of stories of a scaffold shoring system was examined, and a simple 2-D model was developed. It is convenient to analyze or design a scaffold-shoring system using such a simplified structural model. In this paper, a closed-form solution to the 2-D model was obtained. To simplify analysis, a model consisting of a rigid horizontal bar and two vertical bars, with a moment of inertia $\alpha I$ (where $I$ is

the moment of inertia of the original vertical bars), was used to replace the 2-D model. It was shown using FEA that the analytical model exhibited the same structural behavior as the 2-D model when $\alpha$ was equal to 1.54.

Under the assumption that the analytical model buckles at the lowest story, a closed-form solution for the critical loads was derived using a bifurcation approach to the elastic-buckling problem. In this closed-form solution, critical loads are function of the number of stories, material properties, and section properties of the scaffolds. Critical loads and failure modes were compared for scaffold systems from 2 to 20 stories in height obtained using the closed-form solution and the computational solution of the same analytical model. Values obtained using these two different approaches were very close (within 8%). Therefore, Eq. (12) is accepted as a closed-form solution to the analytical model.

## References

Chen, W.F. and Lui, E.M. (1987), *Structural Stability*, Prentice-Hall, Englewood Cliffs, N.J., ISBN 0-13-500539-6.

Huang, Y.L., Cheng, H.J., Rosowsky, D.V. and Kao, Y.G. (2000), "Load-carrying capacities and failure modes of scaffold-shoring systems, Part I: Modeling and experiments", *Structural Engineering and Mechanics*, **10**(1), 53-66.

Jan, T.S. (1987), "General instability of scaffold", *Proceedings of International Conference on Structural Failure*, Singapore.

Peng, J.L., Pan, A.D., Rosowsky, D.V., Chen, W.F., Yen, T. and Chan, S.L. (1996), "High clearance scaffold systems during construction, II: Structural analysis and development of design guidelines", *Engineering Structures*, **18**(3), 258-267.

Yen, T, Chen, H.J., Huang, Y.L., Chen, W.F., Chi, R.C. and Lin, Y.C. (1997), "Design of scaffold shores for concrete buildings during construction", *Journal of the Chinese Institute of Engineers*, **20**(6), 603-614.

## Appendix

Simplification of Eq. (11) to the form shown in Eq. (12):

$$\left[(N-1)\left(\frac{S_{ij}^2}{S_{ii}}-S_{ij}\right)-2(S_{ii}+S_{ij})+N(kL)^2\right]=0$$

$$(N-1)(S_{ij}^2-S_{ii}^2)-2S_{ii}(S_{ii}+S_{ij})+NS_{ii}(kL)^2=0$$

$$S_{ii}=\frac{kL\sin kL-(kL)^2\cos kL}{2-2\cos kL-kL\sin kL}$$

$$S_{ij}=\frac{(kL)^2-kL\sin kL}{2-2\cos kL-kL\sin kL}$$

$$S_{ij}^2-S_{ii}^2=\frac{-2(kL)^3\sin kL+2(kL)^3\sin kL\cos kL+(kL)^4\sin^2 kL}{(2-2\cos kL-kL\sin kL)^2}$$

$$S_{ii}(S_{ii}+S_{ij})=\frac{(kL)^3\sin kL-(kL)^3\sin kL\cos kL-(kL)^4\cos kL+(kL)^4\cos^2 kL}{(2-2\cos kL-kL\sin kL)^2}$$

$$S_{ii}(kL)^2=\frac{(kL)^3\sin kL-(kL)^4\cos kL}{2-2\cos kL-kL\sin kL}$$

$$=\frac{2(kL)^3\sin kL-2(kL)^3\sin kL\cos kL-(kL)^4\sin^2 kL}{(2-2\cos kL-kL\sin kL)^2}$$

$$-\frac{2(kL)^4\cos kL-2(kL)^4\cos^2 kL-(kL)^5\cos kL\sin kL}{(2-2\cos kL-kL\sin kL)^2}$$

$$(N-1)(S_{ij}^2-S_{ii}^2)-2S_{ii}(S_{ii}+S_{ij})+NS_{ii}(kL)^2=0$$

$$(N-1)[-2(kL)^3\sin kL+2(kL)^3\sin kL\cos kL+(kL)^4\sin^2 kL]$$
$$-2[(kL)^3\sin kL-(kL)^3\sin kL\cos kL-(kL)^4\cos kL+(kL)^4\cos^2 kL]$$
$$+N\{[2(kL)^3\sin kL-2(kL)^3\sin kL\cos kL-(kL)^4\sin^2 kL]$$
$$-[2(kL)^4\cos kL-2(kL)^4\cos^2 kL-(kL)^5\cos kL\sin kL]\}=0$$

$$-(kL)^4\sin^2 kL+2(kL)^4\cos kL-2(kL)^4\cos^2 kL-2N(kL)^4\cos kL$$
$$+2N(kL)^4\cos^2 kL+N(kL)^5\cos kL\sin kL=0$$

$$-2(N-1)(kL)^4\cos kL+2(N-1)(kL)^4\cos^2 kL$$
$$+N(kL)^5\cos kL\sin kL-(kL)^4\sin^2 kL=0$$

$$2(N-1)(\cos^2 kL-\cos kL)+N(kL)\cos kL\sin kL-\sin^2 kL=0$$

$$2(N-1)(1-\sec kL)+NkL\tan kL-\tan^2 kL=0$$